

## Dynamic DNA-controlled "stop-and-go" assembly of well-defined protein domains on RNA-scaffolded TMV-like nanotubes

---

Angela Schneider, Fabian J. Eber, Nana L. Wenz, Klara Altintoprak, Holger Jeske, Sabine Eiben\* and Christina Wege\*

Department of Molecular Biology and Plant Virology, Institute of Biomaterials and Biomolecular Systems, University of Stuttgart, Pfaffenwaldring 57, 70569 Stuttgart, Germany

### Supplementary Information

The following data present supplemental results obtained for both TMV-derived RNA scaffolds and the three additional heterologous RNA (hRNA) species including non-TMV sequences, all of them containing the TMV OAs.

**Figure S1** shows the composition of the DNA templates for the hRNA constructs I to III.

**Figures S2 to S7** focus on details of the results obtained for the TMV-based RNA 2253, a scaffold substantially shorter than wt-RNA, and the corresponding expectations. Figure S5 contains additional findings for wt-RNA as it depicts initial experiments on the toehold release of stopper S3' performed with both RNAs employed in the study.

**Figures S8 and S9** depict specifications of the statistical evaluation. They show boxplots for the length distribution analysis of three independent experiments each for the stopped and released particles with wt-RNA and the three hRNA constructs.

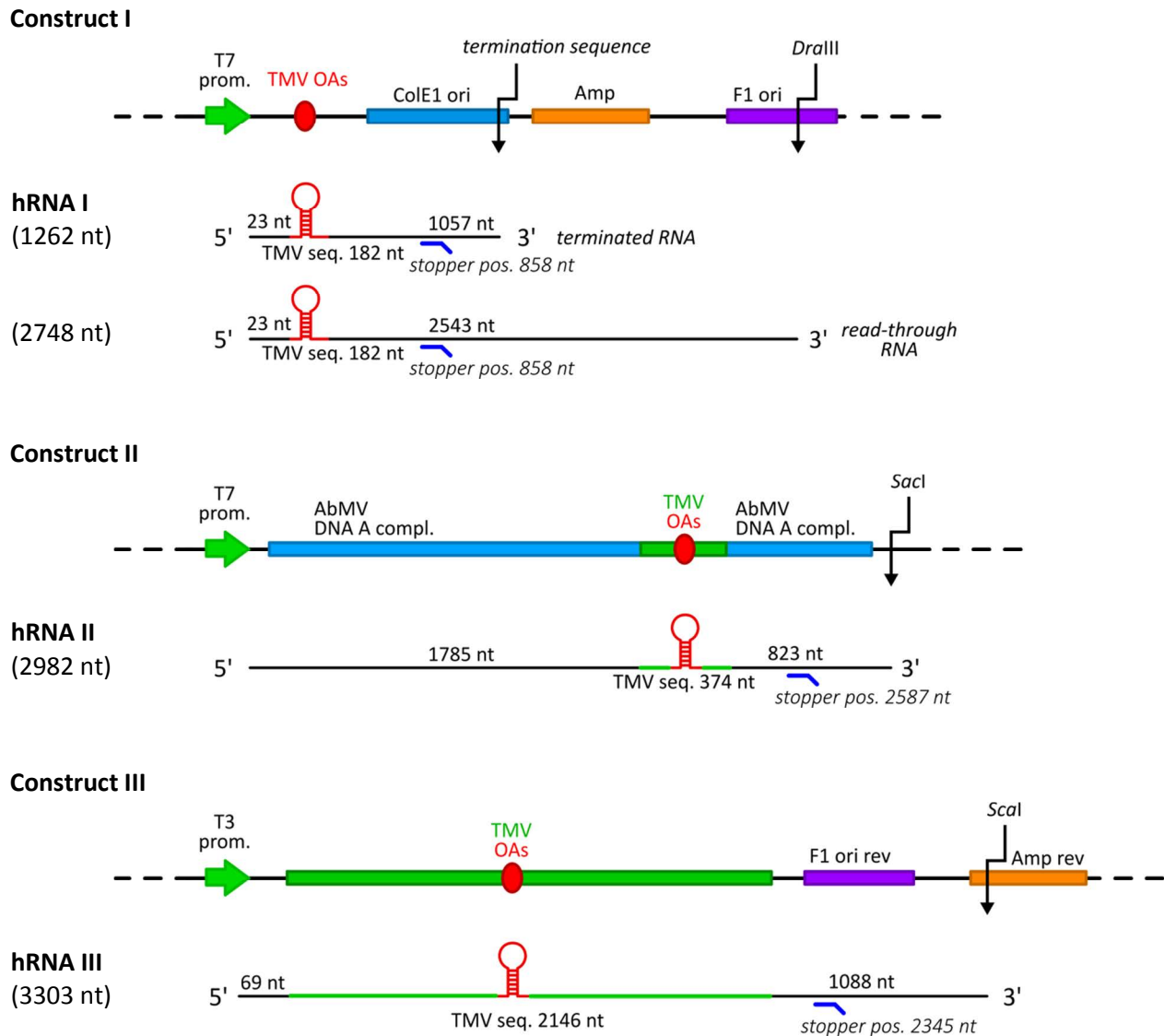


**Figure S1.** Plasmid constructs for *in vitro* transcription to produce the heterologous RNAs (hRNAs). Segments between the relevant T7 or T3 RNA polymerase promoter and the restriction sites used for linearization of the plasmids are shown. Residual TMV sequences are colored green with the OAs in red. Heterologous coding and non-coding sequences of prokaryotic and eukaryotic origin are colored individually (common abbreviations of plasmid elements are used). AbMV DNA A: Abutilon mosaic virus genomic DNA A. Below the plasmid constructs, the expected RNAs are depicted in 5' to 3' orientation, with the lengths of the different sequence elements and the positions of the stopper oligomers (blue kinked lines) indicated. Drawings are not in scale. **Construct I:** TMV OAs sequence inserted into pGEM-T, linearized with DraIII. **Construct II:** TMV portion with OAs in pLitmus 28i combined with most of the (complementary) sequence of a circular ssDNA plant begomovirus DNA A component (Abutilon mosaic virus, AbMV, DNA A), linearized with SacI. **Construct III:** TMV portion with OAs inserted into pBluescript II SK, linearized with ScaI. The opposite orientations of the bacterial sequence elements and the additional ColE1 ori in pGEM-T ensure encapsidation of distinct coding and non-coding RNA sequences of prokaryotic and bacteriophage origin (in constructs I/III), whereas the AbMV DNA elements (in construct II) contain eukaryotic ORF portions in coding and reverse orientation (due to the naturally bidirectional transcription of the circular plant viral DNA) as well as non-coding intergenic regions.

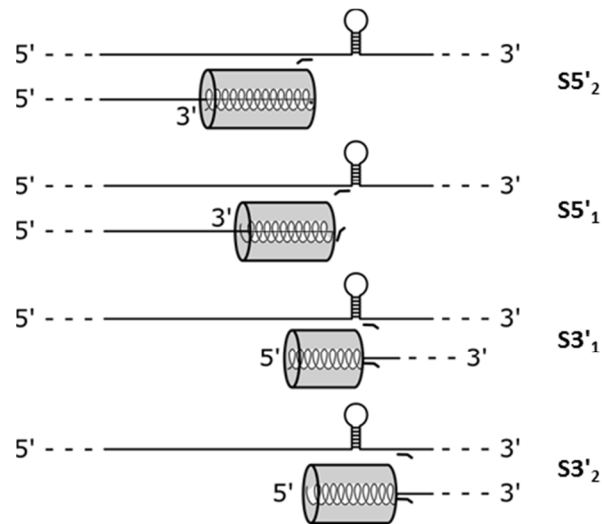


**Figure S2.** Cartoon illustrating the distinct types of stalled nanotubes with a non-encapsitated RNA portion expected to arise upon effective blocking of their assembly by different stoppers, hybridized to sites 5' (upstream) or 3' (downstream) of the OAs on RNA 2253.

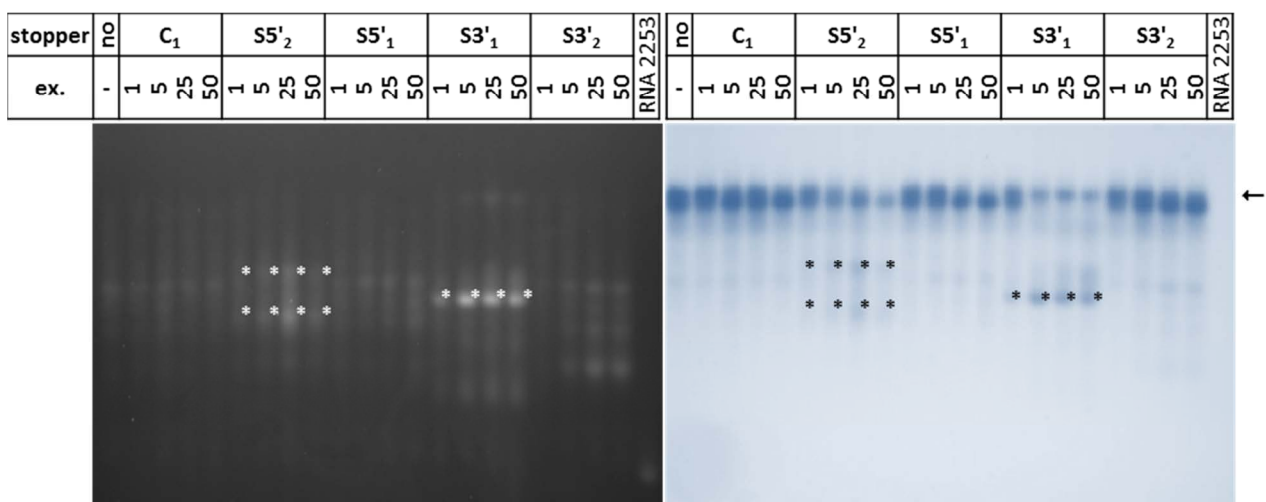


**Figure S3.** "Stop": The influence of distinct stoppers on the self-assembly of TMV CP with RNA 2253, as visualized after nanoparticle separation in a native agarose gel in comparison to control reaction products. Two different control samples were prepared: "no", i.e. fully assembled nanotubes scaffolded by RNA devoid of stoppers, and "C<sub>1</sub>", i.e. fully assembled nanotubes obtained in the presence of a DNA oligomer with no complementarity to the RNA. Hybridization was performed with variable molar excess (ex.) of stopper over RNA for 5 min at 65 °C, cooling to 30 °C with a rate of 1 °C/s, followed by assembly for 7 h at 25 °C. RNA 2253 serves as marker. The gel was first stained with ethidium bromide (left), followed by Coomassie Brilliant Blue-staining (right). The arrow indicates bands of fully assembled tubes of 106 nm length as confirmed by *in vitro* assembled particles without denaturation step (iva). Black/white asterisks (\*) label bands with higher electrophoretic mobility.

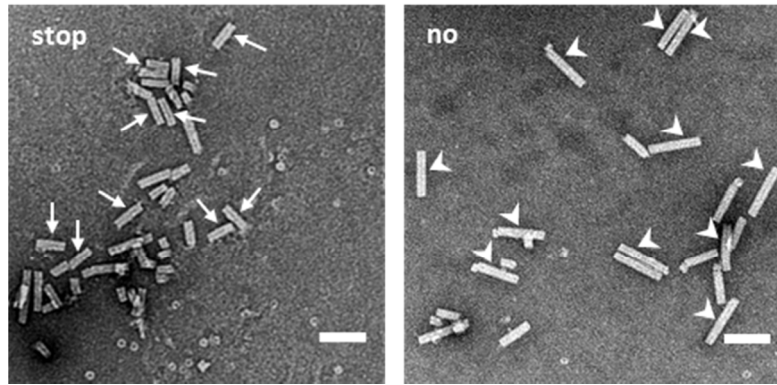


**Figure S4.** Visualizing the "stop" state arisen in the presence of stopper  $S3'_1$  hybridized to RNA 2253 during its self-assembly with TMV CP. TEM analysis of the respective nanotubular products. "Stop": partial, interrupted assembly directed by  $S3'_1$ /RNA. Arrows point at the resulting particles with lengths in the range of 55 to 60 nm. "No": assembly directed by RNA without any stopper. Arrowheads denote fully assembled nanotubes with lengths in the range of 100 to 110 nm. Scale bars: 100 nm.

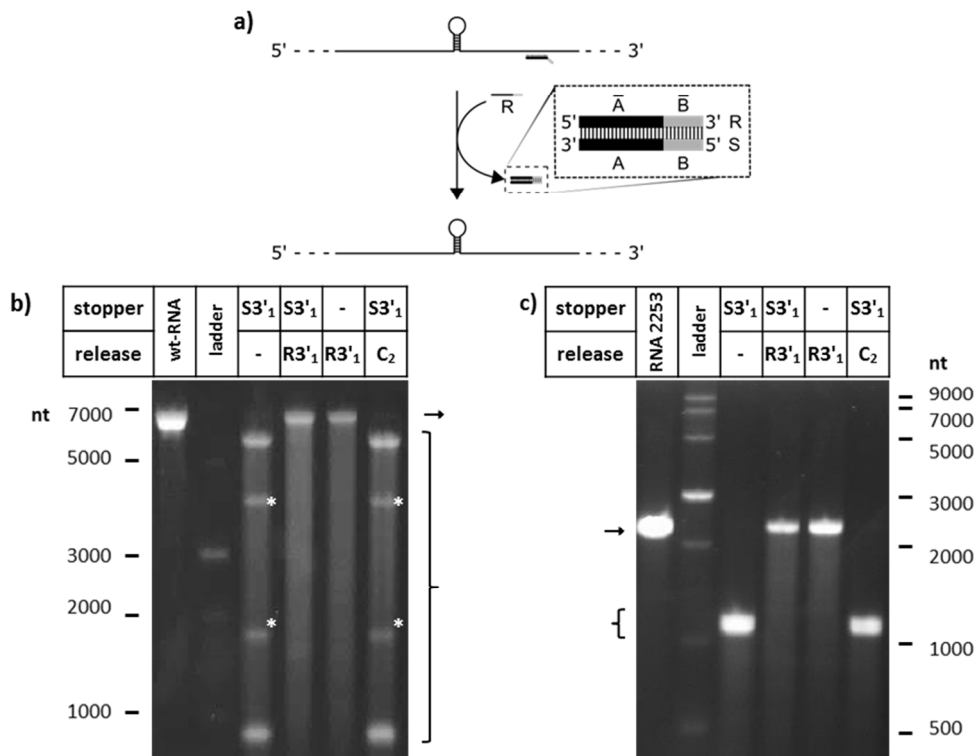


**Figure S5.** Reversibility of stopper  $S3'_1$  hybridization to the RNA scaffolds through its displacement by toehold-release achieved ("fueled") with DNA oligomer  $R3'_1$ . **a)** Scheme of the release process (in the absence of CPs). **b) and c):** Agarose gel electrophoretic separation of the products after RNase H cleavage of DNA/RNA hybridization products of wt-RNA (b) or RNA 2253 (c). Fragments were separated on 1 % or 2 % agarose gels, respectively, under denaturing conditions. Stopper DNA oligomers were hybridized to the RNAs in 5-fold molar excess, prior to RNase H treatment. Arrows denote bands of undigested RNA, brackets the range of fragments expected after digestion. White asterisks label additional fragments occurring upon RNase H incubation.

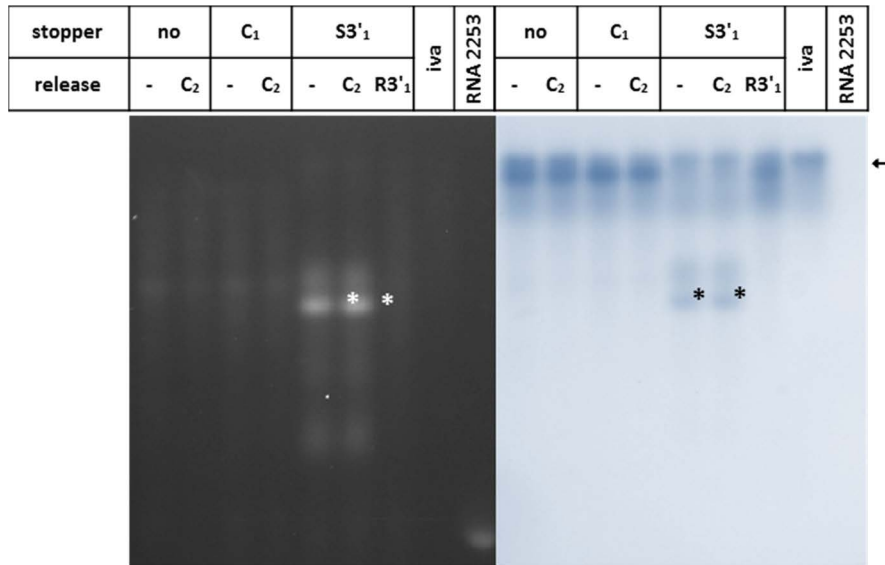


**Figure S6.** "Stop-and-go": controlled stop of the RNA-directed self-assembly of TMV CP by hybridization of stopper S3'<sub>1</sub> to RNA 2253, and its subsequent displacement by toehold-release with the DNA "fuel" oligomer R3'<sub>1</sub>. Native agarose gel of products in the "stop", "release" and "control" reaction states, i.e. after incubation at 25 °C to allow assembly of nucleoprotein tubes in the absence (no) or presence (S3'<sub>1</sub>) of the stopper, or after its subsequent release by a suitable oligomer (R3'<sub>1</sub>). The arrow indicates bands of fully assembled tubes as confirmed by *in vitro* assembled particles without denaturation step (iva). Black/white asterisks (\*) label bands of increased electrophoretic mobility, reflecting stalled nanotubes. RNA 2253 serves as a marker.

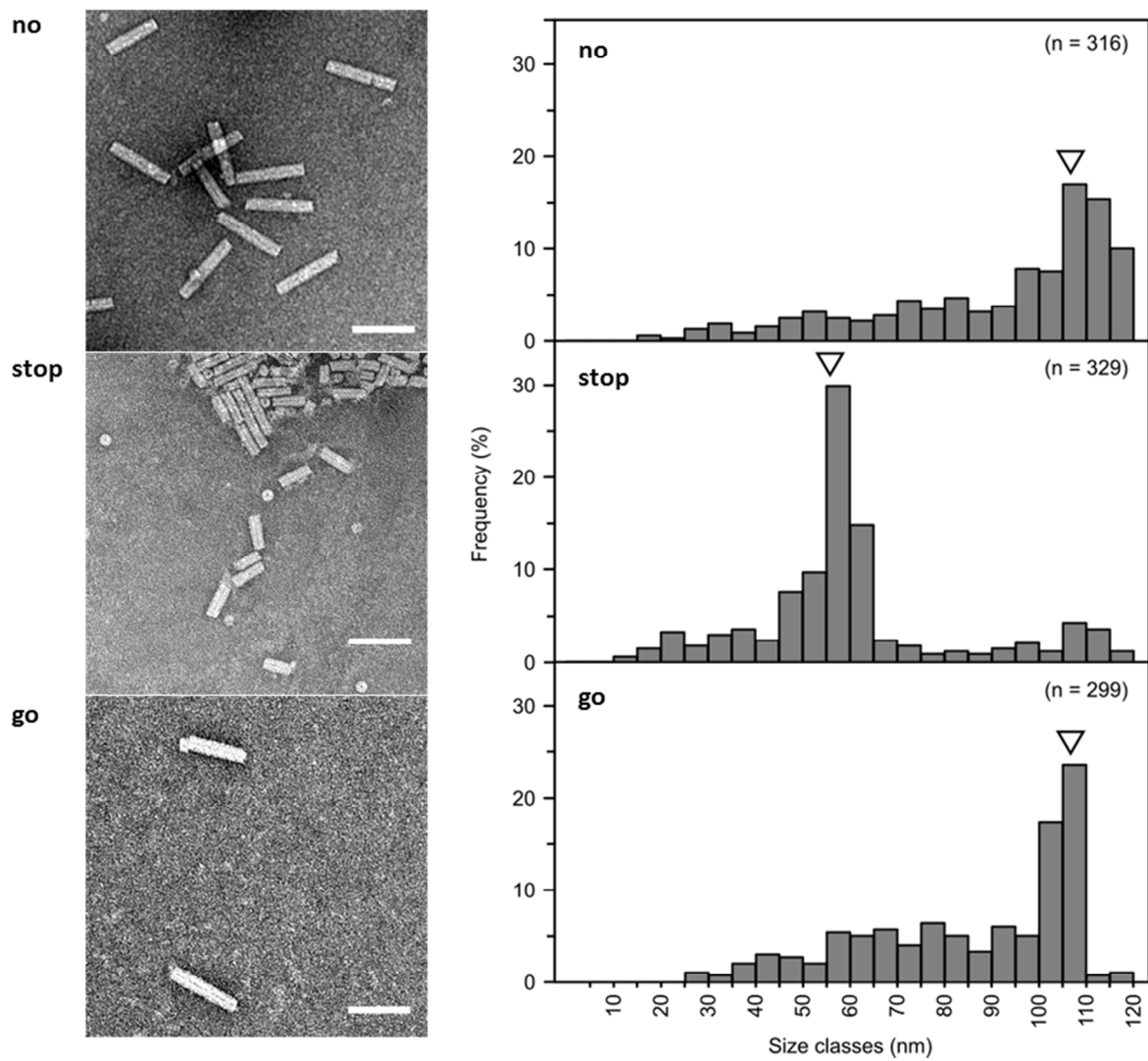


**Figure S7.** "Stop-and-go": Analysis of the resulting nanotube length distributions. "no": assembly directed by RNA 2253 devoid of stopper; "stop": temporarily stopped assembly due to blockage by  $S3'_1$ ; "go": assembly completed after subsequent addition of  $R3'_1$  (to the  $S3'_1$ -stalled partial nanotubes in the presence of free CP). **Left:** TEM images; scale bars: 100 nm. **Right:** Corresponding histograms with  $n$  structures analyzed, triangles indicate the expected nanotube lengths. For details, refer to main article text.

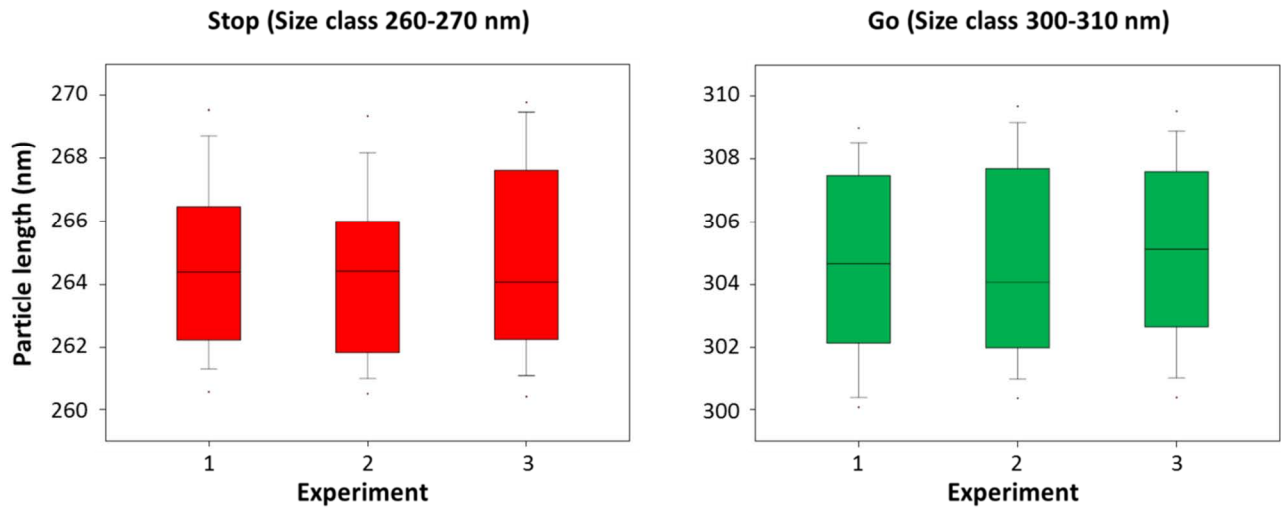


**Figure S8.** "Stop-and-go": Comparative statistical analysis of the "stop"- and "go"-classes obtained in three experiments performed with wt-RNA scaffolds. The expected "stop"-class of 260-270 nm (left) as well as the "go"-class of 300-310 nm (right) length did not differ significantly between all independent experiments ( $p = 0.630$  and  $p = 0.752$ , respectively). Data are presented as boxplots (line: median, box boundaries: 25/75 % quartiles, whiskers: 10/90 % percentiles, dots: 5/95 % percentiles).

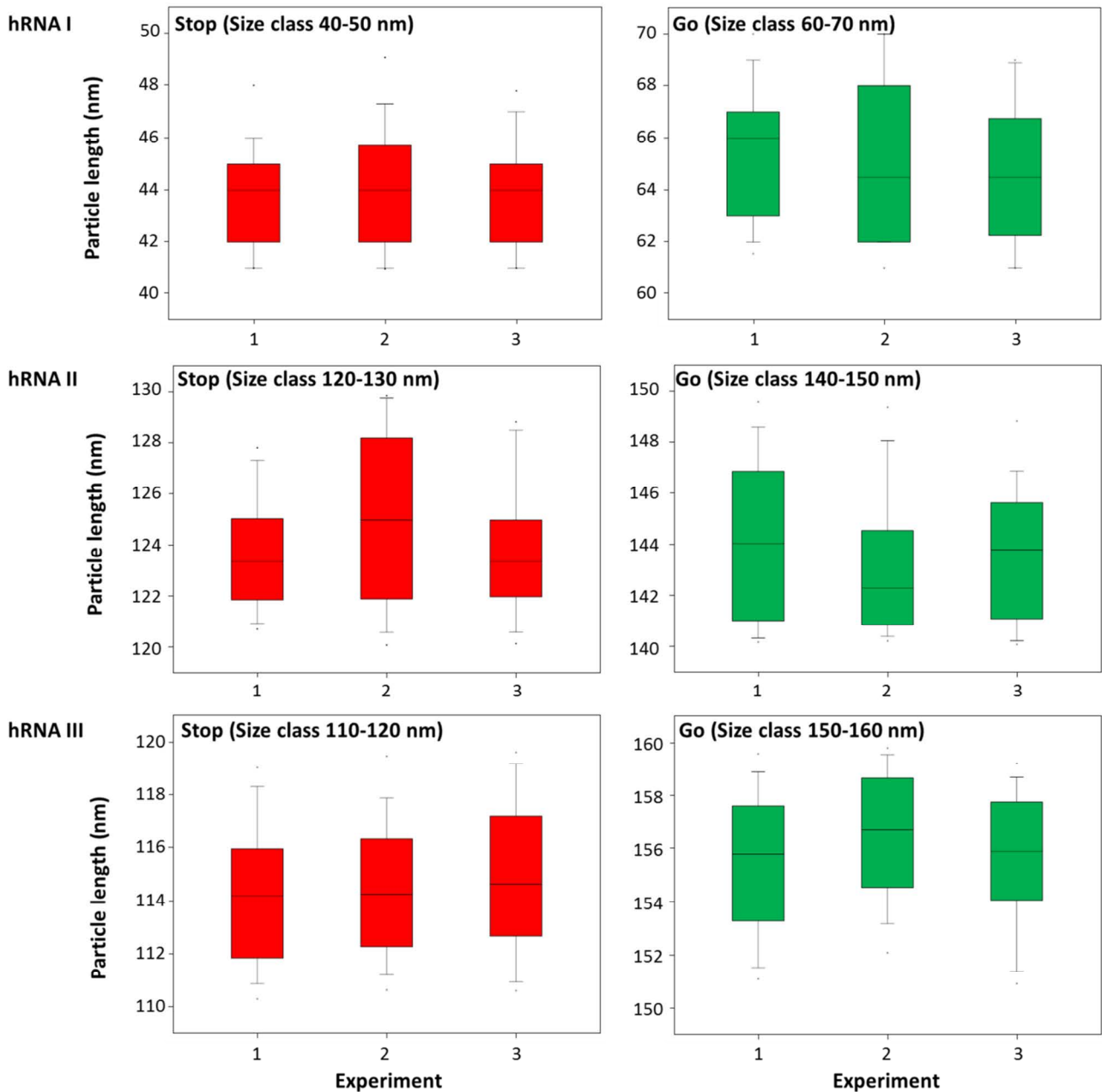


**Figure S9.** "Stop-and-go": Statistical analysis of the "stop"- and "go"-classes obtained in three experiments each performed with three different heterogeneous RNAs. Both the expected "stop"-class (left) and the "go"-class (right) did not differ significantly between the independent experiments for each hRNA. Data are presented as boxplots (line: median, box boundaries: 25/75 % quartiles, whiskers: 10/90 % percentiles, dots: 5/95 % percentiles).

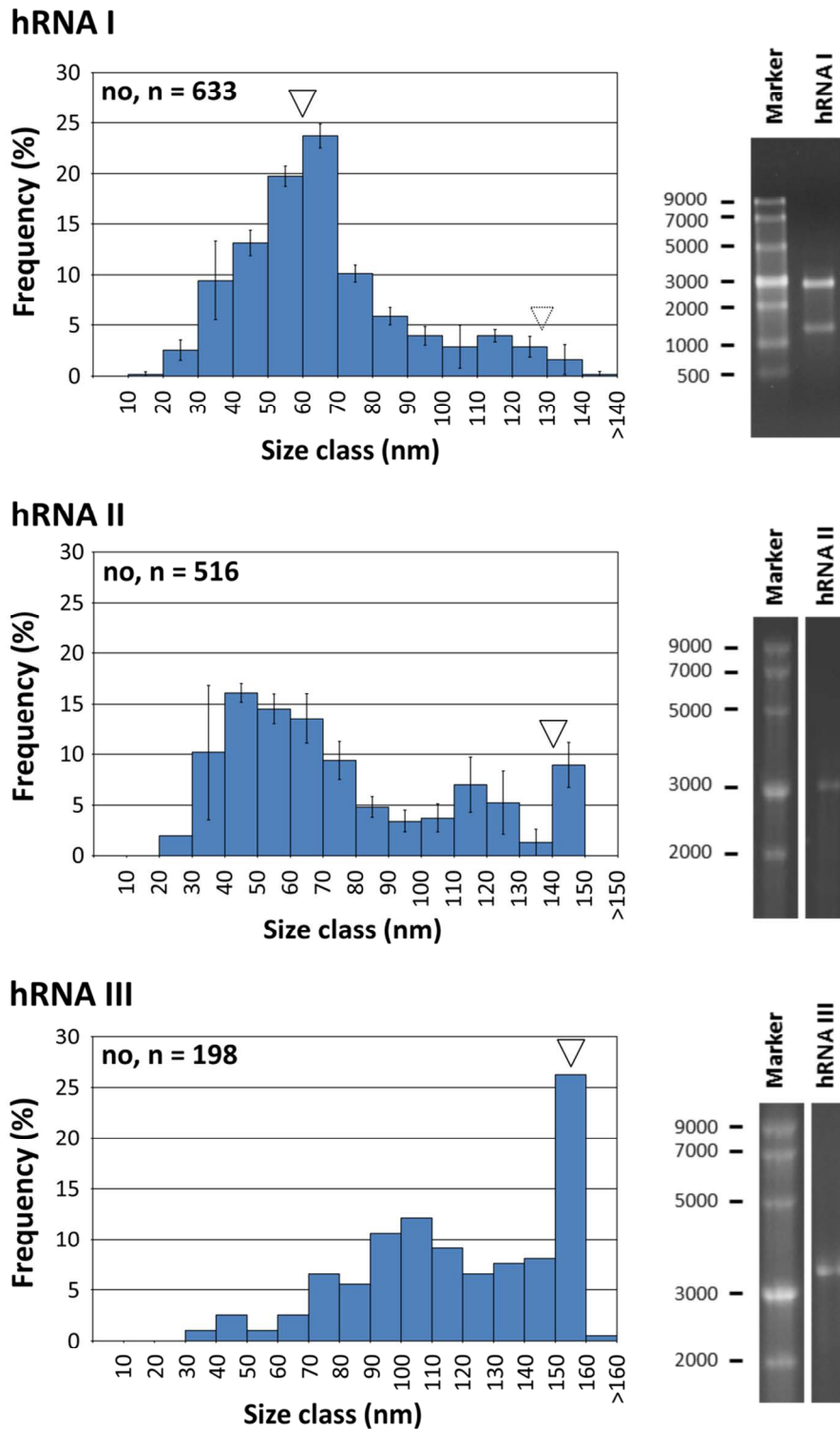


**Figure S10.** Assembly of hRNAs with TMV CP without stopper. Left: Histograms with  $n$  structures analyzed. For hRNAs I and II, the frequencies of three independent experiments were averaged, the error bars show the standard deviations between the datasets. Triangles indicate the expected nanotube lengths. Right: Electrophoretic analyses of the hRNA scaffolds in 1.5 % denaturing agarose gels. For details, namely the presence of two hRNA I subspecies and its effect on nanotube formation (with the larger read-through species accounting for tube lengths up to 130 nm, see dotted triangle), see main text.